PARALLEL MULTI-FREQUENCY NARROWBAND ACTIVE NOISE CONTROL SYSTEMS

F. Yang, A. Gupta, and S. M. Kuo

Vibration and Acoustics Center
Northern Illinois University
DeKalb, IL 60115, USA

ABSTRACT

This paper analyzes and optimizes narrowband active noise control systems using multiple second-order adaptive filters. Theoretical analysis of the overall parallel structure is based on autocorrelation and cross-correlation matrices. Analytical result shows the use of single error signal to update all adaptive filters with different input signals will introduce extra tonal components in the residual noise. An optimized algorithm that uses bandpass filters to split the fullband error signal into multiple bandlimited subband error signals according to the frequencies of reference signals is developed to improve steady-state performance.

Index Terms— Active noise control, adaptive notch filters, parallel structures, multi-frequency narrowband

1. INTRODUCTION

Active noise control (ANC) systems [1] use secondary sources to produce an equal-amplitude but opposite-phase anti-noise to cancel the undesired noise based on acoustic superposition principle. These systems are widely applied in automotives, appliances, industrial, consumer electronics, medical instruments, etc. In many practical applications, noise caused by rotating (or repetitive) machinery such as engines is usually periodic that contains multiple narrowband components at fundamental frequency and its harmonics. The systems used for canceling periodic noises are called narrowband ANC systems.

The single-frequency adaptive notch filter with two adaptive weights, auxiliary reference signal, and a 90°-phase shifter was developed in [2] for canceling an undesired narrowband component. This adaptive notch filter was applied to narrowband ANC [3]. To reduce complexity of implementing Hilbert transformer, a simple delay unit Z^{-1} is used to replace the 90°-phase shifter as shown in Fig. 1 [4]. In the figure, $d(n)$ is the primary noise to be canceled, $e(n)$ is the residual error, $x(n)$ is the reference signal generated by a sine-wave generator, $y(n)$ is the anti-noise output from the adaptive filter, $S(z)$ is the secondary path transfer function, and $\hat{S}(z)$ is the estimated model of $S(z)$.

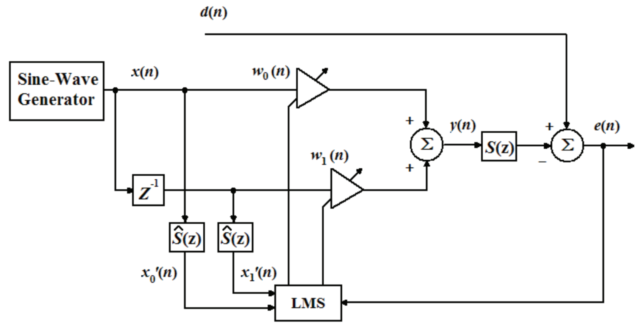

Fig. 1 A single-frequency narrowband ANC system.

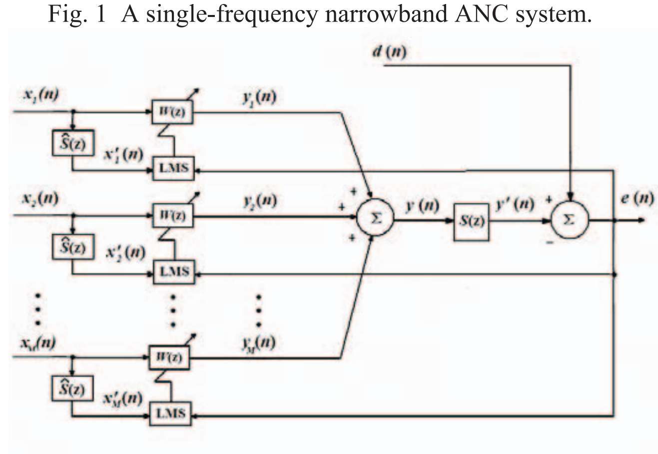

Fig. 2 Parallel multi-frequency narrowband ANC system.

In practice, the periodic noise contains multiple sinusoids with harmonic-related frequencies. A narrowband ANC system that connects multiple adaptive notch filters in parallel for attenuating periodic noise has been developed in [3]. Assuming that the primary noise contains M sinusoidal components, M second-order adaptive notch filters (as shown in Fig. 1) can be connected in parallel to attenuate these sinusoids as illustrated in Fig. 2. Previous works only analyzed convergence and steady-state performance of single-frequency ANC shown in Fig. 1. This paper analyzed the complicated overall parallel structure shown in Fig. 2, and presents a new algorithm to reduce residual noise in steady state.

2. MULTI-FREQUENCY NARROWBAND ANC

The primary signal $d(n)$ contains M sinusoidal components:

$$d(n)=\sum_{m=1}^{M}A_{d,m}\sin(\omega_m n+\phi_{d,m}), \qquad (1)$$

where $A_{d,m}$ and $\phi_{d,m}$ are the magnitude and phase of the sinusoidal components of the primary signal at frequency ω_m. The reference signal consists of M sinusoids generated by respective sinewave generators. Therefore, the reference sinusoid of the mth channel is expressed as

$$x_m(n)=A_m\sin(\omega_m n), \qquad m = 1, 2, \ldots, M. \qquad (2)$$

The filtered-x least-mean-square (FXLMS) algorithm can be expressed as [1]

$$\mathbf{w}_m(n+1)=\mathbf{w}_m(n)+\mu\mathbf{x}'_m(n)e(n), \qquad (3)$$

where $\mathbf{w}_m(n)$ and $\mathbf{x}'_m(n)$ are the weight vector and filtered reference signal vector in the mth channel. The overall output $y(n)$ is the summation of all filter outputs as

$$y(n)=\sum_{m=1}^{M}y_m(n), \qquad m=1, 2, \ldots, M, \qquad (4)$$

where $y_m(n)$ is the ANC output at mth channel as shown in Fig. 2.

The autocorrelation matrix of input signals is

$$\mathrm{R}=\begin{bmatrix}\mathrm{R}_{11} & \mathrm{R}_{12} & \cdots & \mathrm{R}_{1M}\\ \mathrm{R}_{21} & \mathrm{R}_{22} & \cdots & \mathrm{R}_{2M}\\ \vdots & \cdots & \ddots & \vdots\\ \mathrm{R}_{M1} & \mathrm{R}_{M2} & \cdots & \mathrm{R}_{MM}\end{bmatrix}, \qquad (5)$$

where the sub-matrix

$$\mathrm{R}_{pq}=E[\mathrm{x}'_\mathrm{p}(n)\mathrm{x}'^{T}_\mathrm{q}(n)], \qquad p, q = 1, 2, \ldots, M, \qquad (6)$$

is the autocorrelation matrix of two reference sinusoids in the pth and the qth channels. Using the similar analysis techniques for the single-frequency ANC systems [5], we get

$$\mathrm{R}_{pq}=0_{2\times 2}, \qquad p\neq q \text{ and } p, q = 1, 2, \ldots, M, \qquad (7)$$

and

$$\mathrm{R}_{pp}=\frac{A'^2_p}{2}\begin{bmatrix}1 & \cos\omega_p\\ \cos\omega_p & 1\end{bmatrix}, \qquad p = 1, 2, \ldots, M, \qquad (8)$$

where A'_p is the product of the reference sinusoid amplitude A_p and the secondary-path magnitude response $A_{s,p}$ in the pth channel, i.e. $A'_p=A_pA_{s,p}$. Therefore, the autocorrelation matrix is

$$\mathrm{R}=\begin{bmatrix}\mathrm{R}_{11} & & & \\ & \mathrm{R}_{22} & & \\ & & \ddots & \\ & & & \mathrm{R}_{MM}\end{bmatrix}=\Lambda\mathrm{R}_{pp}, \qquad p = 1, 2, \ldots, M, \qquad (9)$$

where Λ denotes the diagonal symbol. The cross-correlation vector p is

$$\mathrm{p}=\begin{bmatrix}\mathrm{p}_1^T & \mathrm{p}_2^T & \cdots & \mathrm{p}_M^T\end{bmatrix}^T, \qquad (10)$$

where the subvector

$$\mathrm{p}_p=E[d(n)\mathrm{x}'_\mathrm{p}(n)], \qquad p = 1, 2, \ldots, M, \qquad (11)$$

represents the crosscorrelation between the primary and reference signals in the pth channel. Similarly, we can have

$$\mathrm{p}_p=\frac{A'_pA_{d,p}}{2}\begin{bmatrix}\cos(\phi_{d,p}-\phi_{s,p})\\ \cos(\omega_p+\phi_{d,p}-\phi_{s,p})\end{bmatrix}, \quad p = 1, 2, \ldots, M, \qquad (12)$$

where $\phi_{s,p}$ is the secondary-path phase response in the pth channel. The optimal weight vector is

$$\mathrm{w}^o=\begin{bmatrix}(\mathrm{w}_1^o)^T & (\mathrm{w}_2^o)^T & \cdots & (\mathrm{w}_M^o)^T\end{bmatrix}^T, \qquad (13)$$

where

$$\mathrm{w}_p^o=\mathrm{R}_{pp}^{-1}\mathrm{p}_p=\frac{A_{d,p}}{A'_p\sin\omega_p}\begin{bmatrix}\sin(\omega_p+\phi_{d,p}-\phi_{s,p})\\ -\sin(\phi_{d,p}-\phi_{s,p})\end{bmatrix}, \quad p = 1, 2,\ldots, M. \qquad (14)$$

The eigenvalues of each sub-matrix R_{pp} are

$$\lambda_{l,p}=\frac{A'^2_p}{2}(1\pm\cos\omega_p), \quad l = 0, 1 \text{ and } p = 1, 2,\ldots, M. \qquad (15)$$

Assume the maximum and minimum eigenvalues are

$$\lambda_{\max.}=\frac{A'^2_k}{2}(1+|\cos\omega_k|) \qquad (16)$$

$$\lambda_{\min.}=\frac{A'^2_h}{2}(1-|\cos\omega_h|), \qquad (17)$$

the eigenvalue spread becomes

$$\rho=\frac{\lambda_{\max.}}{\lambda_{\min.}}=\frac{A'^2_k(1+|\cos\omega_k|)}{A'^2_h(1-|\cos\omega_h|)}. \qquad (18)$$

It shows that the secondary path transfer function also affects the convergence rate. Based on this observation, an improved FXLMS algorithm for the multiple-frequency ANC system in parallel structure was developed in [6] to improve the convergence of FXLMS algorithm.

3. EFFECTS OF USING SINGLE ERROR SIGNAL

The magnitude spectrum of the error signal shows that extra harmonics are induced during the procedure of convergence, regardless of the conventional or the improved FXLMS algorithm [7, 8]. This phenomenon is studied and an optimized method is proposed.

3.1. Analysis of error effects

The error signal of the narrowband ANC system with the FXLMS algorithm can be expressed as

$$e(n)=d(n)-\sum_{m=1}^{M}\sum_{l=0}^{1}w_{m,l}(n)x'_m(n-l). \qquad (19)$$

With Eq. (3) and the initial condition $w_{m,l}(0)=0$, the filter coefficients at time N+1 can be expressed as

$$w_{m,l}(N+1)=\sum_{n=1}^{N}\mu x'_m(n-l)e(n), \quad l=0, 1;\ m=1, 2,\ldots, M. \qquad (20)$$

The error signal become

$$e(N=1)=d(N+1)-\mu\sum_{m=1}^{M}\sum_{l=0}^{1}\sum_{n=1}^{N}x'_m(n-l)x'_m(N+1-l)e(n)\cdot \quad (21)$$

Eq. (1) shows the primary noise $d(n)$ does not include any component at frequencies other than ω_m, m=1, 2,…, M. Therefore, the extra harmonics in the residual error at time N+1 can only originate from $y'(N+1)$. Given the reference signal defined in (2) and using the trigonometry, we obtain

$$y'(N+1)=\mu\sum_{m=1}^{M}\sum_{l=0}^{1}\sum_{n=1}^{N}\frac{A'^2_m}{2}\{\cos[\omega_m(N+1-n)]-\cos[\omega_m(N+1+n-2l)+2\phi_{s,m}]\}e(n)\cdot \quad (22)$$

Without loss of generality, assume the common error $e(n)$ can be expressed as

$$e(n)=\sum_{m=1}^{M}A_{e,m}(n)\sin[\omega_m n+\phi_{e,m}(n)]+r(n),\ m=1, 2,\dots, M, \quad (23)$$

where $A_{e,m}(n)$ and $\phi_{e,m}(n)$ are time-variable amplitude and phase at frequency ω_m at time n, and $r(n)$ is an arbitrary unknown signal which can contain periodic components at frequencies other than ω_m, m=1, 2,…, M. Also, assume that

$$P_1=\cos[\omega_m(N+1-n)] \quad (24)$$

$$P_2=\cos[\omega_m(N+1+n-2l)+2\phi_{s,m}],\ m=1, 2,\dots, M. \quad (25)$$

Then,

$$P_1e(n)=\cos[\omega_m(N+1-n)]\left\{\sum_{m=1}^{M}A_{e,m}(n)\sin[\omega_m n+\phi_{e,m}(n)]+r(n)\right\}=Q_1+Q'_1 \quad (26)$$

where

$$Q_1=\frac{A_{e,p}}{2}(n)\{\sin[\omega_m(N+1)+\phi_{e,p}(n)]+\sin[\omega_m(2n-N-1)+\phi_{e,p}(n)]\} \quad (27)$$

$$Q'_1=\sum_{p=1,p\neq m}^{M}\frac{A_{e,p}}{2}(n)\sin[\omega_p n+\omega_m(N+1-n)+\phi_{e,p}(n)] \quad (28)$$
$$+\sum_{p=1,p\neq m}^{M}\frac{A_{e,p}}{2}(n)\sin[\omega_p n-\omega_m(N+1-n)+\phi_{e,p}(n)]+\cos[\omega_m(N+1-n)]r(n)\cdot$$

Similarly, we can have

$$P_2e(n)=\cos[\omega_m(N+1+n-2l)+2\phi_{s,m}]\left\{\sum_{m=1}^{M}A_{e,m}(n)\sin[\omega_m n+\phi_{e,m}(n)]+r(n)\right\}=Q_2+Q_2' \quad (29)$$

where

$$Q_2=\frac{A_{e,p}}{2}(n)\{\sin[\omega_m(N+1+2n-2l)+2\phi_{s,m}+\phi_{e,p}(n)]+\sin[\omega_m(2l-N-1)-2\phi_{s,m}+\phi_{e,p}(n)]\} \quad (30)$$

$$Q'_2=\sum_{p=1,p\neq m}^{M}\frac{A_{e,p}}{2}(n)\sin[\omega_p n+\omega_m(N+1+n-2l)+2\phi_{s,m}+\phi_{e,p}(n)] \quad (31)$$
$$+\sum_{p=1,p\neq m}^{M}\frac{A_{e,p}}{2}(n)\sin[\omega_p n-\omega_m(N+1+n-2l)-2\phi_{s,m}+\phi_{e,p}(n)]+\cos[\omega_m(N+1+n-2l)]r(n)\cdot$$

Therefore,

$$P_1-P_2=(Q_1-Q_2)+(Q'_1-Q'_2) \quad (32)$$

and

$$y'(N+1)=\mu\sum_{m=1}^{M}\sum_{l=0}^{1}\sum_{n=1}^{N}\frac{A'^2_m}{2}(Q_1-Q_2)+\mu\sum_{m=1}^{M}\sum_{l=0}^{1}\sum_{n=1}^{N}\frac{A'^2_m}{2}(Q'_1-Q'_2)\cdot \quad (33)$$

Equations (27) and (30) show that Q_1 and Q_2 only contain harmonics related to frequency ω_m, while Eqs. (28) and (31) show that Q'_1 and Q'_2 contain harmonics related to many other frequencies. Therefore, the first part on the right-hand side of Eq. (33) contributes to the components related to the M basic frequencies of the anti-noise, and the second part indicates the extra unrelated harmonics induced in the residual error signal.

3.2. An optimized method

The extra unrelated harmonics induced in the error signal result from using the single error signal to update all parallel filters. These extra harmonics can be reduced by introducing a bandpass filter at each channel to obtain individual error signals for updating filter coefficients. Figure 3 shows the block diagram of the optimized method for the parallel multi-frequency narrowband ANC system.

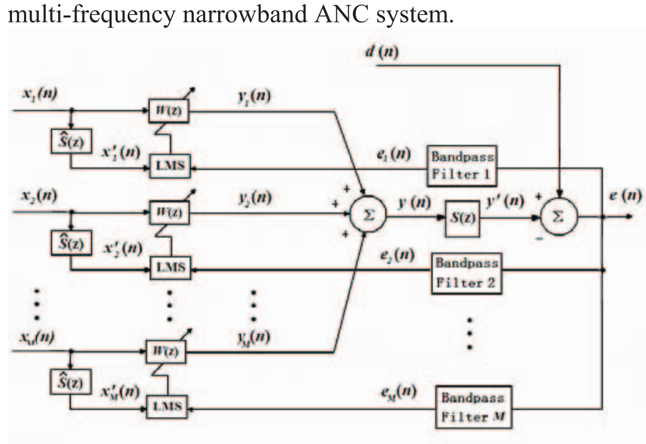

Figure 3 An optimized method for the multi-frequency narrowband ANC system.

The FXLMS algorithm for this method becomes

$$\mathrm{w}_m(n+1)=\mathrm{w}_m(n)+\mu\mathrm{x}'_{\mathrm{m}}(n)e_m(n),\ m=1, 2,\dots, M, \quad (34)$$

where

$$e_m(n)=A_{e,m}(n)\sin[\omega_m n+\phi_{e,m}(n)],\ m=1, 2,\dots, M, \quad (35)$$

is the individual error signal in the mth channel. It can be proved that both Q'_1 and Q'_2 as defined in Eqs. (28) and (31) are zero. Consequently, at time N+1,

$$y'(N+1)=\mu\sum_{m=1}^{M}\sum_{l=0}^{1}\sum_{n=1}^{N}\frac{A'^2_m}{2}(Q_1-Q_2)\cdot \quad (36)$$

This shows that the extra unrelated harmonics are reduced. From the previous sections, it is known that the convergence speed of the FXLMS algorithm depends on the eigenvalue spread of the input autocorrelation matrix and the response of secondary path transfer function. Therefore, the optimized method will not affect the convergence rate.

4. COMPUTER SIMULATIONS

Computer simulations are used to compare the optimized method with the conventional one. The algorithm used for simulation is the improved FXLMS algorithm developed in [6]. Figures 4 and 5 illustrate the spectra of error signal before (Fig. 4) and after (Fig. 5) the algorithm has converged. The upper plot shows the improved method with bandpass filters and the lower plot shows original algorithm without bandpass filters. In each plot, the solid line shows the spectrum of primary signal and the dashed line shows the spectrum of error signal. Figure 4 shows that bandlimited error signals reduced extra harmonics at high frequency range before the convergence of the algorithm, and Figure 5 shows the optimized algorithm effectively reduced extra harmonic at the low frequency range after the algorithm has converged.

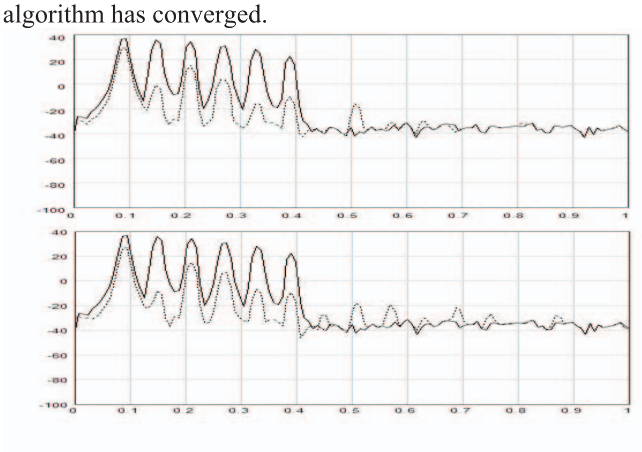

Figure 4 Spectrum of residual error signal at time n=2000. Magnitude unit in y-axis is dB, and frequency ω in x-axis is π rad/s.

5. CONCLUSIONS

This paper analyzed the multi-frequency narrowband ANC systems in parallel form using the FXLMS algorithm. Convergence was analyzed using eigenvalue and eigenvector techniques. It is also found that when a single error signal is used to update all the adaptive filters, extra harmonics at unrelated frequencies will be induced in the error signal. An optimized method in which bandpass filters are used to split error signal into subband signals has been proposed. Computer simulations show that this proposed method is effective in reducing the extra unrelated harmonics and does not affect the convergence speed.

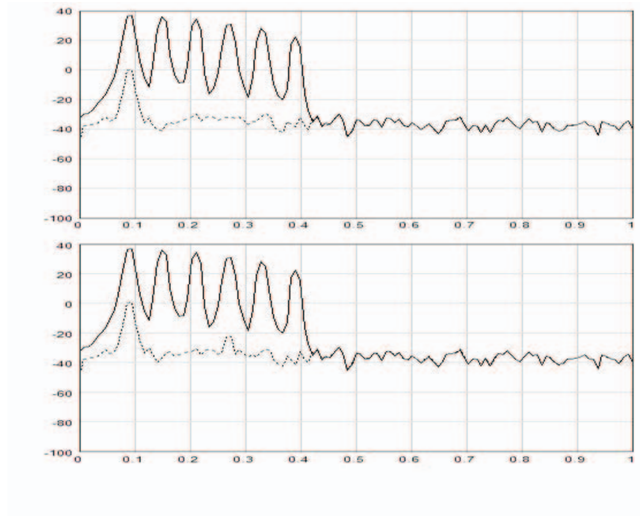

Figure 5 Spectrum of error signal at time n=6000. Magnitude unit in y-axis is dB, and frequency ω in x-axis is π rad/s.

6. REFERENCES

[1] S.M. Kuo and D.R Morgan, *Active Noise Control Systems–Algorithms and DSP Implementations*, New York, NY: John Wiley & Sons, 1996.

[2] B. Widrow et al., "Adaptive noise canceling: Principles and applications," *Proc. IEEE*, vol. 63, pp. 1692-1716, Dec. 1975.

[3] E. Ziegler, "Selective active cancellation systems for repetitive phenomena," U.S. patent no. 4,878,188, 1989.

[4] S.M. Kuo, S. Zhu, and M. Wang, "Development of optimum adaptive notch filter for fixed-point implementation in active noise control," in *Proc. Int. Conf. Industrial Electronics*, pp. 1376-1378, 1992.

[5] S.M. Kuo and A.B. Puvvala, "Effects of frequency separation in periodic active noise control systems," *IEEE Trans. Audio, Speech, and Language Processing*, vol. 14, no. 5, pp. 1857-1866, 2006.

[6] S.M. Kuo, M. Tahernezhadi, and W. Hao, "Convergence analysis of narrowband active noise control systems," *IEEE Trans. on Circuits and Systems*, vol. 46, no 2, pp. 220-223, Feb. 1999.

[7] F.C. Yang, *An Analysis of Narrowband Active Noise Control Systems Using Parallel Adaptive Notch Filters*, MS Thesis, Northern Illinois University, May 2007.

[8] F.C. Yang, A. Gupta, and S.M. Kuo, "Analysis of narrowband active noise and vibration control systems using parallel adaptive notch filters," *J. of Vib. and Control*, vol. 14, pp. 931-951, 2008.